Theoretical differential and total cross sections of water-molecule ionization by electron impact

C. Champion, J. Hanssen, and P. A. Hervieux
Laboratoire de Physique Moléculaire et des Collisions, Institut de Physique, 1 Boulevard Arago, Technopôle 2000, 57078 Metz Cedex 3, France

(Received 16 July 2001; published 16 January 2002)

In the present paper, triply, doubly, singly, and total cross sections of the vapor water-molecule ionization are calculated in the distorted-wave Born approximation, without exchange. In these conditions, fair agreements are found with experimental data, specially in the low and intermediate ejected energy domain ($E_e < E_s$, where E_e and E_s are the ejected and scattered energy, respectively), and an extensive comparison between experimental and theoretical results is given in terms of differential and total cross sections. The present results are also compared to other theoretical ones, specially to results obtained in the plane-wave Born approximation, and in the first-Born approximation frameworks, in order to underline the distortion effect.

DOI: 10.1103/PhysRevA.65.022710 PACS number(s): 34.80.Dp

I. INTRODUCTION

Understanding the complex interactions that are involved when atoms or molecules are ionized by electron impact remains one of the greatest challenges facing atomic physics at the present time. In effect, besides its fundamental aspect, specially in the study of the electronic structure of the target, it is a powerful tool for the study of the mechanisms of ionization itself, whose comprehension becomes important in many domains, such as plasma physics, fusion experiments, astrophysics, and even in the study of ionizing collisions on living matter. These interactions have been studied for many years, and both a theoretical understanding and experimental techniques have been made (see, for example, [1,2] and references therein). The most sophisticated of the past experiments have studied the ionization reaction by measuring the resulting products in coincidence. For single ionization by electron impact, the $(e,2e)$ coincidence experiment probes the scattered and ejected electron momenta that result from the ionization events. By selecting different momenta at which the outgoing electrons are observed, a complete description of the ionization process can be obtained in principle. In spite of the considerable body of experimental $(e,2e)$ studies on many atomic targets (in the domain of the electron momentum spectroscopy [2] and for lower incident-energy values for symmetric and nonsymmetric situations [3]), the ionization processes are experimentally less studied on molecular (polyatomic) systems [4–9]. The case of the water molecule is even more dramatic since we find in the literature very rare experimental studies dedicated to doubly differential cross section (DDCS) measurements. We can cite the extensive work given by Opal *et al.* [10], who provides doubly and singly ionization cross sections for an incident energy $E_a = 500\,\mathrm{eV}$ in a range of ejected energies $E_e = 4.13\text{–}205\,\mathrm{eV}$ and ejection angles $\theta_e = 30° - 180°$, and the work of Bolorizadeh and Rudd [11] and of Oda [12] dedicated to energetic electrons with an incident energy $E_a = 500\,\mathrm{eV}$. Concerning singly differential cross sections (SDCS's) and total cross sections (TCS's), the literature is more abundant and we find several experimental works for a large range of incident energies [13–24].

On the theoretical side, the most recent study on the general subject of molecular ionization by electron impact (with a section dedicated to water ionization) has been published by Kim [25–27] who developed a ''binary-encounter-dipole model'' that combines the binary-encounter theory of Vriens [28] with the dipole interaction of the Bethe theory [29] for fast incident electrons. However, this work gives only a semiclassical description of the ionization process in using average quantities such as kinetic energy of the target electrons of each subshell and differential dipole-oscillator strengths for the corresponding molecular orbital (MO). Moreover, these calculations are only limited to singly differential and total-ionization cross sections.

In the past, quantum-mechanical studies of the vapor water ionization were already given [30–32] but remain largely limited to the plane-wave Born approximation (PWBA). Moreover, these results are only in qualitative agreement with the experimental data; indeed, these theories overestimate in general the total-ionization cross sections. Thus, in absence of theoretical quantum-mechanical investigations, which are quite involved, several semiempirical approaches have been developed [33–36]. Consequently, the present work appears as a detailed theoretical study of the ionization process of the vapor water-molecule by electron impact. Furthermore, our theoretical approach may be easily introduced in numerical simulations such as the Monte Carlo track structure code for electrons in water [37] or in matter in general. Indeed, for these codes, multiple differential calculations represent useful input data in order to describe in detail all the ionizing events, in terms of energy deposits and angular distributions. In this context, the ionization cross sections at all energies of incident particles and ejected electrons are needed to follow the history of an incident particle and its products for all ranges of energy transferred in individual collisions. Under these conditions, we have recently presented in a previous paper [38] a theoretical study dedicated to the influence of the water-molecule target orientation on the differential cross sections in pointing out the huge discrepancies observed between the eightfold differential cross sections (8DCS's) calculated for a particular molecular orientation [defined by the Euler angles $(\alpha;\ \beta;\ \gamma)$] and the corresponding 5DCS's (i.e., the 8DCS's averaged over all the available molecular orientations).

In the same state of mind, we propose by the present work a detailed description of a more sophisticated approach de-

veloped in the distorted-wave Born approximation (DWBA) framework to provide useful differential and total ionization cross section calculations. The initial state is described as a product of a plane-wave function (for the incident electron) with a molecular-wave function described by a linear combination of atomic orbitals (LCAO's), all centered on the heavy oxygen atom (the self-consistent-field LCAO MO method, [39]). The ejected electron (which is by definition the slowest particle in the final state) is described by a distorded-wave function, whereas the scattered electron is described by a plane-wave function. A comparison of the present results with other theoretical ones performed in the PWBA and in the first-Born approximation (FBA) frameworks will be exposed in the following in order to outline the importance of the distortion effect. Finally, the differential cross sections will be integrated over the scattered or ejected solid angle, and over the energy transfer, in order to obtain successively the SDCS's and the TCS's, which will be compared to an extensive set of experimental data and to other theoretical model predictions [25,32] (see [40] for a complete review of the cross section sets available in the literature).

The present paper is organized as follows. Our theoretical approach is outlined in Sec. II, and the results concerning multiple differential and total cross section calculations are given and analyzed in Sec. III. In Sec. III A, we will define two types of DDCS's: a first one plotted versus the scattered angle, and a second one versus the ejected angle that will be compared to the rarely available DDCS experimental measurements. In Sec. III B, the SDCS's are presented, analyzed, and compared to an extensive set of experimental data, and a particular attention is finally paid to the TCS's that are presented in Sec. III C. Finally a conclusion is given in Sec. IV. Atomic units are used throughout unless otherwise indicated.

II. THEORETICAL METHOD

As described in [38], the nonrelativistic 8DCS's of the water-molecule ionization are, for a given molecular orientation [defined by the Euler angles $(\alpha;\beta;\gamma)$], expressed by

$$\left[\frac{d^8\sigma}{d\Omega_s\, d\Omega_e\, dE_e\, d\alpha\, d\beta\, d\gamma}\right](\alpha;\beta;\gamma) = \sum_{j=1}^{N_{\mathrm{MO}}}\left[\frac{d^8\sigma}{d\Omega_s\, d\Omega_e\, dE_e\, d\alpha\, d\beta\, d\gamma}\right]_j(\alpha;\beta;\gamma) = \frac{1}{(2\pi)^5}\sum_{j=1}^{N_{\mathrm{MO}}}\frac{k_e k_s}{k_a}|[T_{ab}(\alpha;\beta;\gamma)]_j|^2, \quad (1)$$

where the transition amplitude T_{ab} is given by

$$[T_{ab}(\alpha;\beta;\gamma)]_j = \frac{4\pi}{q^2}\langle \mathcal{F}^{(j)(-)}_{\mathbf{k}_e}(\mathbf{r})|e^{i\mathbf{q}\cdot\mathbf{r}}|\Psi_j(\mathbf{r})\rangle, \quad (2)$$

with the momentum transfer $\mathbf{q}$ defined by $\mathbf{q}=\mathbf{k}_a-\mathbf{k}_s$ (see Fig. 1 for more details).

$N_{\mathrm{MO}}=5$ is the number of molecular orbitals of the water-molecule description proposed by Moccia [39]. Each of them, denoted Ψ_j, is expressed in terms of Slater-like functions all centered at a common origin (for more details see [38] and [39]). Concerning the final state, the ejected electron is described by a distorted-wave function, whereas in [38] a Coulomb wave function was used. $\mathcal{F}^{(j)(-)}_{\mathbf{k}_e}(\mathbf{r})$ represents the continuum distorted-wave function of ejected momentum $\mathbf{k}_e$, and as we will see in the following, it depends on the MO.

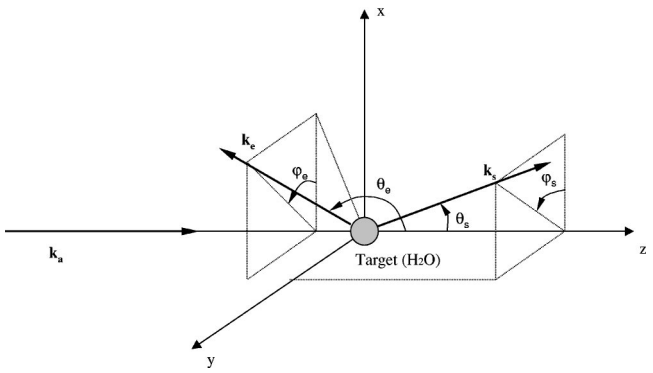

FIG. 1. Reference frame of the ionizing collision of a water target. $\mathbf{k}_a$, $\mathbf{k}_s$, and $\mathbf{k}_e$ represent the wave vectors of the incident, scattered, and ejected electrons, respectively. The corresponding polar and azimuthal angles are denoted (θ_s,φ_s) and (θ_e,φ_e), respectively.

The calculation of the transition amplitude T_{ab} [Eq. (2)] is performed in using the partial-wave expansion method. Thus, $\mathcal{F}^{(j)(-)}_{\mathbf{k}_e}(\mathbf{r})$ and the plane-wave function $e^{i\mathbf{q}\cdot\mathbf{r}}$ can be written, respectively, as

$$\mathcal{F}^{(j)(-)}_{\mathbf{k}_e}(\mathbf{r}) = \sum_{l_e=0}^{\infty}\sum_{m_e=-l_e}^{+l_e}(4\pi)(i)^{l_e}\exp[-i(\sigma_{l_e}+\delta^{(j)}_{l_e})] \times\frac{F^{(j)}_{l_e}(k_e;r)}{k_e r}Y^*_{l_e m_e}(\hat{\mathbf{k}}_e)Y_{l_e m_e}(\hat{\mathbf{r}}) \quad (3)$$

and

$$e^{i\mathbf{q}\cdot\mathbf{r}} = \sum_{l=0}^{\infty}\sum_{m=-l}^{+l}(4\pi)i^l j_l(qr)Y^*_{lm}(\hat{\mathbf{q}})Y_{lm}(\hat{\mathbf{r}}), \quad (4)$$

where the quantum numbers (l_e,m_e) correspond to the ejected electron, and where the quantities $j_l(r)$ and $Y_{lm}(\hat{\mathbf{r}})$ correspond to the Bessel functions and the spherical harmonics, respectively. σ_{l_e} is the Coulomb phase shift, whereas $\delta^{(j)}_{l_e}$ represents the short-range phase shift associated to the distortion potential.

The radial function $F^{(j)}_{l_e}(k_e;r)$ introduced in Eq. (3) is the solution of the differential equation

$$\left[\frac{1}{2}\frac{d^2}{dr^2}+E_e-\frac{l_e(l_e+1)}{2r^2}-\tilde{V}_j(r)\right]F^{(j)}_{l_e}(k_e;r)=0 \quad (5)$$

and exhibits an asymptotic behavior given by

$$F_{l_e}^{(j)}(k_e;r)\sim\sin\left(k_e r-l_e\frac{\pi}{2}-\eta_e\ln(2k_e r)+\sigma_{l_e}+\delta_{l_e}^{(j)}\right), \tag{6}$$

where $\eta_e=-1/k_e$ is the Sommerfeld parameter.

The total distortion potential $\tilde{V}_j(r)$ introduced in Eq. (5) is orbital dependent and is given by

$$\tilde{V}_j(r)=\tilde{V}_j^{\rm elec}(r)+\tilde{V}^{\rm ion}(r). \tag{7}$$

The first term corresponds to the electronic contribution, whereas the second one concerns the ionic contribution. They are, respectively, given by

$$V_j^{\rm elec}(\mathbf{r})=\sum_{i=1}^{N_{\rm MO}} N_{ij}\int \Psi_i^*(\mathbf{r}')\frac{1}{|\mathbf{r}-\mathbf{r}'|}\Psi_i(\mathbf{r}')d\mathbf{r}', \tag{8}$$

with

$$N_{ij}=\begin{cases}2 & \text{if } i\neq j,\\ 1 & \text{if } i=j\end{cases} \tag{9}$$

and

$$V^{\rm ion}(\mathbf{r})=-\frac{8}{r}-\frac{1}{|\mathbf{r}-\mathbf{r}_{\rm OH_1}|}-\frac{1}{|\mathbf{r}-\mathbf{r}_{\rm OH_2}|}, \tag{10}$$

where $\|\mathbf{r}_{\rm OH_1}\|=\|\mathbf{r}_{\rm OH_2}\|=R_{\rm OH}=1.814$ a.u. (see Table II in [38]).

The radial potentials $\tilde{V}_j^{\rm elec}(r)$ and $\tilde{V}^{\rm ion}(r)$ used in Eq. (7) are obtained by using the spherical average approximation. In these conditions, the electronic contribution is written as

$$\begin{aligned}\tilde{V}_j^{\rm elec}(r)&\equiv\frac{1}{4\pi}\int V_j^{\rm elec}(\mathbf{r})d\hat{\mathbf{r}}\\ &=\sum_{i=1}^{N_{\rm MO}} N_{ij}\sum_{kk'} a_{ik}a_{ik'}\delta(m_{ik}-m_{ik'})\delta(l_{ik}-l_{ik'})\\ &\quad\times\int_0^\infty R_{n_{ik}l_{ik}}^{\xi_{ik}}(r')\frac{r'^2}{r_>}R_{n_{ik'}l_{ik'}}^{\xi_{ik'}}(r')dr',\end{aligned} \tag{11}$$

where $r_>=\max(r,r')$ and $r_<=\min(r,r')$. (a_{ik},ξ_{ik}) are the coefficients introduced in the LCAO developed by Moccia to describe the molecular-wave function Ψ_i. Similarly, the radial potential $\tilde{V}^{\rm ion}(r)$ is given by

$$\tilde{V}^{\rm ion}(r)\equiv\frac{1}{4\pi}\int V^{\rm ion}(\mathbf{r})d\hat{\mathbf{r}}=-\frac{8}{r}-\frac{2}{R_>}, \tag{12}$$

where $R_>=\max(r,R_{\rm OH})$.

Finally, taking the direction of the initial momentum $\mathbf{k}_a$ to be along the z axis (see Fig. 1) we obtain, for the molecular state labeled j, the following expression of the 8DCS's:

$$\begin{aligned}&\left[\frac{d^8\sigma}{d\Omega_s\,d\Omega_e\,dE_e\,d\alpha\,d\beta\,d\gamma}\right]_j(\alpha;\beta;\gamma)\\ &=\frac{32}{q^4}\frac{k_s}{k_a k_e}\sum_{k,k'=1}^{N_j}\sum_{\mu_k=-l_{jk}}^{+l_{jk}}\sum_{\mu_{k'}=-l_{jk'}}^{+l_{jk'}} a_{jk}a_{jk'}\\ &\quad\times\mathcal{D}^{(l_{jk})}_{\mu_k m_{jk}}(\alpha;\beta;\gamma)\mathcal{S}^{\mu_k}_{n_{jk}l_{jk}}[\mathcal{D}^{(l_{jk'})}_{\mu_{k'}m_{jk'}}(\alpha;\beta;\gamma)\mathcal{S}^{\mu_{k'}}_{n_{jk'}l_{jk'}}]^*,\end{aligned} \tag{13}$$

where N_j is the number of atomic states included in the molecular state j. $\mathcal{S}^{\mu_k}_{n_{jk}l_{jk}}$ is given by

$$\begin{aligned}\mathcal{S}^{\mu_k}_{n_{jk}l_{jk}}&=\sum_{l_e=0}^{\infty}\sum_{m_e=-l_e}^{+l_e}\sum_{l=0}^{\infty} i^{(l-l_e)}\exp[i(\sigma_{l_e}+\delta_{l_e}^{(j)})]\\ &\quad\times\mathcal{A}^{l_{jk}\mu_k}_{l_e m_e l}\mathcal{R}^{n_{jk}l_{jk}}_{ll_e}Y_{l_e m_e}(\hat{\mathbf{k}}_e)Y_{l\mu_k-m_e}(\hat{\mathbf{q}}),\end{aligned} \tag{14}$$

where $\mathcal{A}^{l_{jk}\mu_k}_{l_e m_e l}$ and the radial integration $\mathcal{R}^{n_{jk}l_{jk}}_{ll_e}$ are, respectively, defined by

$$\mathcal{A}^{l_{jk}\mu_k}_{l_e m_e l}=(\hat{l}_{jk}\hat{l}_e\hat{l})^{1/2}\begin{pmatrix}l_{jk} & l_e & l\\ 0 & 0 & 0\end{pmatrix}\begin{pmatrix}l_{jk} & l_e & l\\ \mu_k & -m_e & m_e-\mu_k\end{pmatrix}, \tag{15}$$

with $\hat{l}=2P+1$, and

$$\mathcal{R}^{n_{jk}l_{jk}}_{ll_e}=\int_0^\infty R_{n_{jk}l_{jk}}^{\xi_{jk}}(r)j_l(qr)F_{l_e}^{(j)}(k_e;r)r\,dr, \tag{16}$$

$\mathcal{R}^{\xi_{jk}}_{n_{jk}l_{jk}}(r)$ being the radial part of each atomic orbital implied in the LCAO given by Moccia. By using the orthogonality relation of the rotation matrix $\mathcal{D}^l_{m_1m_2}$ (see [38] for more details), we obtain the following 5DCS's:

$$\begin{aligned}&\left[\frac{d^5\sigma}{d\Omega_s\,d\Omega_e\,dE_e}\right]\\ &=\sum_{j=1}^{N_{\rm MO}}\left[\frac{d^5\sigma}{d\Omega_s\,d\Omega_e\,dE_e}\right]_j\\ &=\frac{1}{8\pi^2}\sum_{j=1}^{N_{\rm MO}}\int\int\int\left[\frac{d^8\sigma}{d\Omega_s\,d\Omega_e\,dE_e\,d\alpha\,d\beta\,d\gamma}\right]_j(\alpha;\beta;\gamma)\\ &\quad\times d\alpha\,d\gamma\sin\beta\,d\beta\\ &=\frac{32}{q^4}\sum_{j=1}^{N_{\rm MO}}\frac{k_s}{k_a k_e}\sum_{k=1}^{N_j}\frac{[a_{jk}]^2}{\hat{l}_{jk}}\sum_{\mu_k=-l_{jk}}^{l_{jk}}|\mathcal{S}^{\mu_k}_{n_{jk}l_{jk}}|^2.\end{aligned} \tag{17}$$

Triply differential cross sections are finally obtained by either integrating the 5DCS's over the ejected or the scattered solid angle, and are denoted $\sigma^{(3)}(E_e,\Omega_s)$ or $\sigma^{(3)}\times(E_e,\Omega_e)$, respectively. Whereas the first ones are obtained analytically, the second one can only be calculated by numerical integration procedures. We have, respectively,

$$\sigma^{(3)}(E_e,\Omega_s)=\left[\frac{d^3\sigma}{d\Omega_s\,dE_e}\right]=\sum_{j=1}^{N_{\rm MO}}\int\left[\frac{d^5\sigma}{d\Omega_s\,d\Omega_e\,dE_e}\right]_j d\Omega_e$$
$$=\sum_{j=1}^{N_{\rm MO}}\left(\frac{8}{\pi}\right)\frac{k_s}{k_a k_e}\frac{1}{q^4}\sum_{k=1}^{N_j}[a_{jk}]^2\sum_{l_e l}\hat{l}_e\hat{l}$$
$$\times\begin{pmatrix} l_e & l & l_{jk}\\ 0 & 0 & 0\end{pmatrix}^2[\mathcal{R}^{n_{jk}l_{jk}}_{ll_e}]^2$$
$$\equiv\sum_{j=1}^{N_{\rm MO}}\sigma_j^{(3)}(E_e,\Omega_s) \tag{18}$$

and

$$\sigma^{(3)}(E_e,\Omega_e)=\left[\frac{d^3\sigma}{d\Omega_e\,dE_e}\right]$$
$$=\sum_{j=1}^{N_{\rm MO}}\int_0^{2\pi}d\varphi_s\int_{+1}^{-1}\left[\frac{d^5\sigma}{d\Omega_s\,d\Omega_e\,dE_e}\right]_j d(\cos\theta_s)$$
$$\equiv\sum_{j=1}^{N_{\rm MO}}\sigma_j^{(3)}(E_e,\Omega_e). \tag{19}$$

The two quantities (18) and (19) are independent of φ_s and φ_e, respectively. Consequently, the DDCS's are proportional to the TDCS's and are defined as

$$\sigma^{(2)}(E_e,\theta_s)=\left[\frac{d^2\sigma}{d(\cos\theta_s)dE_e}\right]$$
$$=\sum_{j=1}^{N_{\rm MO}}\int_0^{2\pi}\left[\frac{d^3\sigma}{d\Omega_s\,dE_e}\right]_j d\varphi_s$$
$$=\sum_{j=1}^{N_{\rm MO}}2\pi\sigma_j^{(3)}(E_e,\Omega_s)\equiv\sum_{j=1}^{N_{\rm MO}}\sigma_j^{(2)}(E_e,\theta_s) \tag{20}$$

and

$$\sigma^{(2)}(E_e,\theta_e)=\left[\frac{d^2\sigma}{d(\cos\theta_e)dE_e}\right]$$
$$=\sum_{j=1}^{N_{\rm MO}}\int_0^{2\pi}\left[\frac{d^3\sigma}{d\Omega_e\,dE_e}\right]_j d\varphi_e$$
$$=\sum_{j=1}^{N_{\rm MO}}2\pi\sigma_j^{(3)}(E_e,\Omega_e)\equiv\sum_{j=1}^{N_{\rm MO}}\sigma_j^{(2)}(E_e,\theta_e). \tag{21}$$

Singly differential cross sections are finally obtained by numerical integration of Eq. (20) or Eq. (21)

$$\left[\frac{d\sigma}{dE_e}\right]=\sum_{j=1}^{N_{\rm MO}}\int_{+1}^{-1}\sigma_j^{(2)}(E_e,\theta_s)d(\cos\theta_s)$$
$$=\sum_{j=1}^{N_{\rm MO}}\int_{+1}^{-1}\sigma_j^{(2)}(E_e,\theta_e)d(\cos\theta_e)\equiv\sum_{j=1}^{N_{\rm MO}}\sigma_j^{(1)}. \tag{22}$$

Then, the total ionization cross sections are given by

$$\sigma=\sum_{j=1}^{N_{\rm MO}}\int_0^{(E_a-V_j)/2}\left[\frac{d\sigma}{dE_e}\right]_j dE_e\equiv\sum_{j=1}^{N_{\rm MO}}\sigma_j, \tag{23}$$

where V_j is the ionization potential of the jth ionized MO (see Table I in [38]).

III. RESULTS

To simplify the presentation of our results, let us first of all define the different independent variables implied in the water-molecule ionization process. Figure 1 shows the different polar (θ_s,θ_e) and azimuthal (φ_s,φ_e) angles in a right-hand reference frame, where the direction of the incident electron is that of the z axis, and the plane formed by $\mathbf{k}_a$ and $\mathbf{k}_s$, the xz plane ($\varphi_s=0$); the labels a, e, and s corresponding to the incident, ejected, and scattered species, respectively.

In the following, we have computed differential and total ionization cross sections for incident energies E_a ranging from 20 eV to 2 keV and values of the energy of the ejected electron E_e varying from 0 to $E_e^{\max}$ with $E_e^{\max}=(E_a-V_i)/2$.

A. Doubly differential cross sections

As explained above in the theoretical section, there are two manners in which to define DDCS's. A first one, called $\sigma^{(2)}(E_e,\theta_s)$, consists in studying the role of the scattered electron, whereas a second one, called $\sigma^{(2)}(E_e,\theta_e)$, concerns the distribution of the ejected electron. In what follows, we present successively these two types of DDCS calculations, the second ones being compared to available experimental data taken from Opal *et al.* [10] (see Sec. III A 2).

1. Variation with the scattering angle θ_s

Figures 2(a)–2(c) display, for an incident energy $E_a=100$ eV, the evolution of $\sigma^{(2)}(E_e,\theta_s)$ for three different energy transfers (dependent on the MO), namely, $\Delta E_a=E_e+V_i$ with $E_e=0.027$, 17.32, and 43.25 eV, respectively. The contribution of each of the four MO's implied in the ionization is outlined in the figures. In the three cases the overall behavior is the same and corresponds to DDCS's extremely peaked at the origin $\theta_s=0°$. The contribution of the three outer molecular subshells is approximately the same since the corresponding ionization potentials are very close. However, for more important energy transfers such as in the case in Fig. 2(c) ($E_e=43.25$ eV), the inner subshell $2A_1$ makes a greater contribution than the other MO, essentially for large values of θ_s, which is what corresponds to smaller impact parameter collisions. In Figs. 2(d) and 2(g), the energy transfer remains very small and the DDCS's' behavior is the same

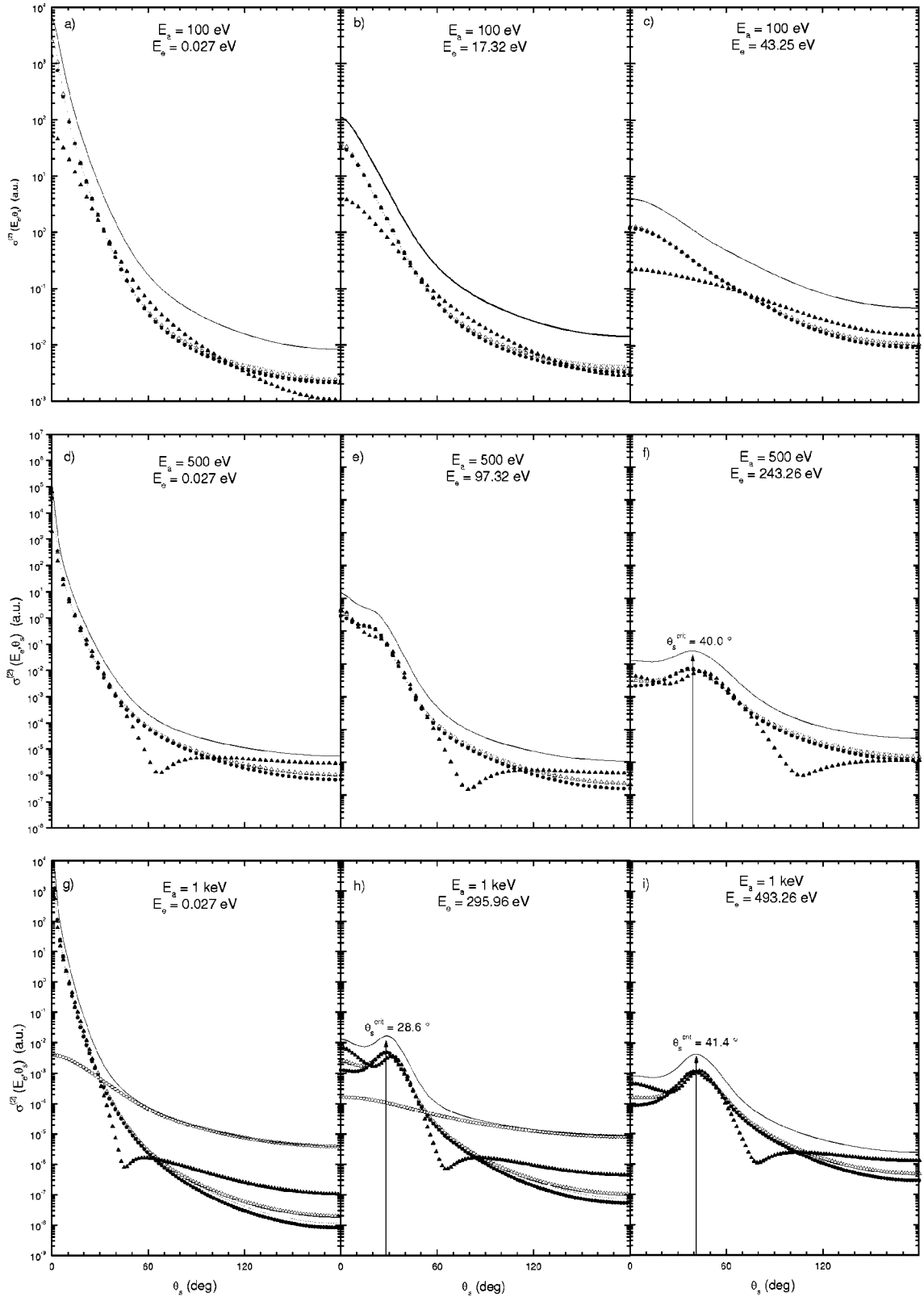

FIG. 2. DDCS's of the vapor water-molecule ionization (expressed in atomic units) plotted versus the scattered angle θ_s for different energetic conditions: first $E_a = 100$ eV with $E_e = 0.027$, 17.32, and 43.25 eV in (a), (b), and (c), respectively; second $E_a = 500$ eV with $E_e = 0.027$, 97.32, and 243.26 eV in (d), (e), and (f), respectively; and third $E_a = 1$ keV with $E_e = 0.027$, 295.96, and 493.26 eV in (g), (h), and (i), respectively. The different subshell contributions are represented: the first MO ($1B_1$) by a dotted line, the second MO ($3A_1$) by open up triangles, the third MO ($1B_2$) by solid circles, the fourth MO ($2A_1$) by solid up triangles, and the fifth MO ($1A_1$) by open circles [only in (g) and (h)]. The solid line corresponds to the ''total'' water-molecule results.

TABLE I. Comparison between the calculated values and the values obtained in the $\sigma^{(2)}(E_e,\theta_s)$ calculations (reported in parentheses) concerning the critical angle θ_s^{crit} corresponding to the binary peak. The contribution of each molecular orbital is evaluated, and we have reported the corresponding value observed for the water molecule.

	$2A_1$	$1B_2$	$3A_1$	$1B_1$	Water molecule
Ionization potential (a.u.)	1.3261	0.6814	0.5561	0.4954	
$E_a=18.38$, $E_e=8.94$ (a.u.)	41.85°	44.18°	44.20°	44.20°	
	(45.7°)	(40.2°)	(38.8°)	(38.7°)	(40.0°)
$E_a=36.76$, $E_e=18.13$ (a.u.)	44.57°	44.60°	44.60°	44.60°	
	(44.1°)	(40.0°)	(39.9°)	(39.8°)	(41.4°)

as cited above. However, in Figs. 2(f) and 2(i) (where E_e is equal to 243.26 and 493.26 eV, respectively), we observe the appearance of a peak centered at a θ_s^{crit} value of about 40° and 41.4°, respectively. In fact, for high velocities of ejection of the molecular electron (i.e., for large ΔE_a values), the angular distribution does not fall off uniformly with the scattered angle but displays maximum for a critical angle θ_s^{crit}, which is what corresponds to binary collision in which the energy lost by the incident electron is completely transferred to the target molecular electron with the residual ion acting as a spectator [41,42]. This is the region of the Bethe ridge that is simply defined by

$$q^2=k_e^2, \tag{24}$$

where the momentum transfer **q** is related to the scattered angle θ_s by

$$q^2=k_a^2+k_s^2-2k_ak_s\cos\theta_s, \tag{25}$$

what implies a θ_s^{crit} value defined by

$$\theta_s^{\text{crit}}=\cos^{-1}\left[\frac{k_a^2+k_s^2-k_e^2}{2k_ak_s}\right]. \tag{26}$$

This quantity depends of the ionized MO and we have reported in the Table I the different θ_s^{crit} calculated values [according to Eq. (26)] compared to the values obtained in the DDCS calculations, for the four MO's implied in the collisions studied in Figs. 2(f) and 2(i).

2. Variation with the ejected angle θ_e

In Figs. 3(a) and 3(b), we have compared our DDCS calculations, called $\overline{\sigma^{(2)}}(E_e,\theta_e)$ and defined as $\overline{\sigma^{(2)}}(E_e,\theta_e)=\sigma^{(2)}(E_e,\theta_e)/2\pi$, to the experimental results taken from Opal *et al.* [10] (open circles) and from Bolorizadeh and Rudd [11] (solid circles) for two incident energy conditions: (a) $E_a=500$ eV and (b) $E_a=1$ keV. We observe a reasonable agreement between the experimental and theoretical results in the two cases, in the small angle region ($\theta_e<60°$), as well for small as for large ejection energies, except maybe for $E_e=40$ eV [Fig. 3(a)], where our results overestimate the experimental ones. However, for $\theta_e>60°$, the agreement becomes more acceptable and we observe, as in the experimental case, the appearance of the binary peak located at the expected θ_e^{crit} value, namely, 51.0° and 63.2° for $E_a=500$ eV, $E_e=100$ eV and $E_a=1$ keV, $E_e=100$ eV, respectively.

By comparison, we have reported in Fig. 3(a) the theoretical results (dashed line) obtained by Long *et al.* [32] in the framework of the density functional theory [11] for $E_a=500$ eV and $E_e=40$ eV. We observe fair agreements be-

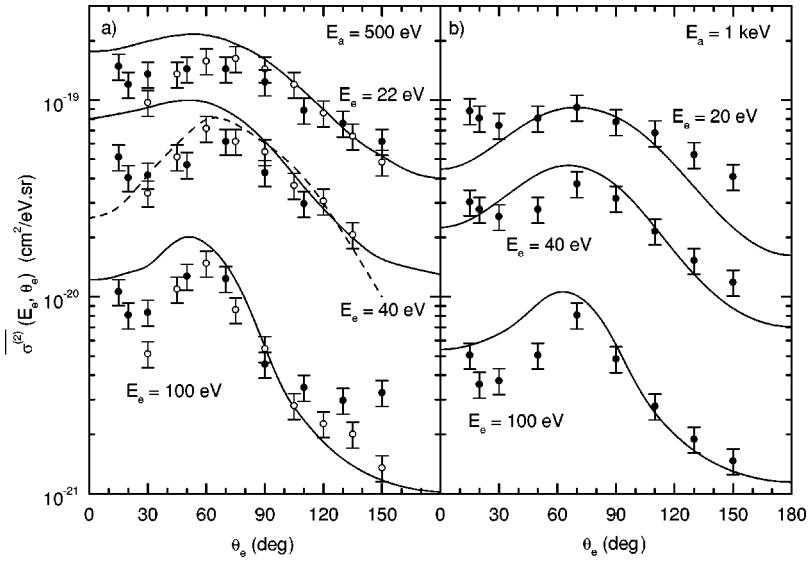

FIG. 3. DDCS's of the vapor water-molecule ionization $[\overline{\sigma^{(2)}}(E_e,\theta_e)]$ calculated from the 5DCS's by numerical integration over the scattered solid angle Ω_s, and averaged over the ejected azimuthal angle φ_e in order to be compared to the experimental data taken from Bolorizadeh and Rudd (solid circles) and from Opal *et al.* (open circles). In the first case, the ejection energy E_e is equal to 22, 40, and 100 eV, successively, whereas, in the second case, the ejection energy E_e is equal to 20, 40, and 100 eV, respectively. (a) and (b) correspond to an incident energy $E_a=500$ eV and $E_a=1$ keV, respectively. The DWBA results are represented by a solid line. In (a) we have reported the results obtained by Long *et al.* for $E_e=40$ eV (dashed line).

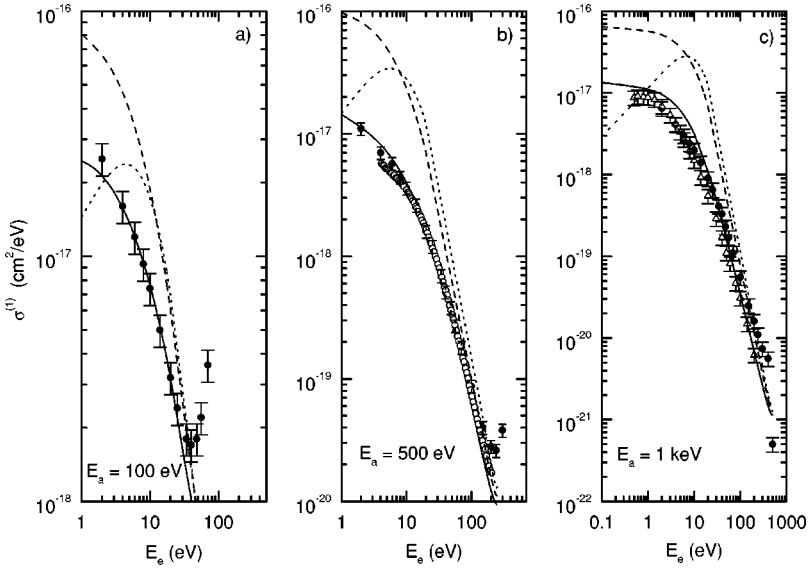

FIG. 4. SDCS's of the vapor water-molecule ionization calculated in the DWBA framework (solid line) compared to FBA and PWBA results (dashed line and dotted line, respectively) in three energetic conditions: (a) $E_a = 100$ eV, (b) $E_a = 500$ eV, and (c) $E_a = 1$ keV. The experimental data reported are taken from Opal *et al.* (open circles), from Bolorizadeh and Rudd (solid circles), and from Vroom and Palmer (open triangles), respectively.

tween these results and ours, specially for large θ_e values (i.e., $\theta_e > 60°$).

B. Singly differential cross sections

In the following we present SDCS calculations for incident energies covering a large range (E_a varying from 50 eV to 2 keV) and for ejected energies varying from 0 to $(E_a - V_i)/2$, in order to take into account the indistinguishability between the ejected and the scattered electron in the final state. Thus, the comparisons between the experimental and the theoretical results will be displayed and discussed only in the first half of the ejection energy range $[0:(E_a - V_i)/2]$ domain that is the most important for the total ionization cross section calculation (see below for the numerical procedure of TCS calculation).

Figures 4(a)–4(c) display singly differential cross sections for three different incident energies, namely $E_a = 100$ eV, $E_a = 500$ eV, and $E_a = 1$ keV, respectively. The results obtained in the DWBA framework are represented by a solid line, whereas the FBA and the PWBA results are represented by a dashed line and a dotted line, respectively. The experimental data reported are taken from Opal *et al.* [10] (open circles), Bolorizadeh and Rudd [11] (solid circles), and from Vroom and Palmer [20] (open triangles), respectively. In all these experiments, the SDCS results are obtained by numerical integration of the measured DDCS's [i.e., the $\overline{\sigma^{(2)}}(E_e, \theta_e)$ presented above], over the ejection solid angle Ω_e. We observe fair agreements between experimental data and the DWBA results, whereas the other theories tend to overestimate them, specially the FBA theory that exhibits a similar overall behavior but large discrepancies at small energy transfers (small ejection energies E_e). Concerning the PWBA results, we observe a maximum sited at $E_e = 4$, 6, and 8 eV, for $E_a = 100$ eV, 500 eV, and 1 keV, respectively, a maximum that does not exist in the experimental measurements. For large energy transfer values (namely E_e in the order of about $E_a/2$), the different theories tend to be identical.

Figure 5 displays the DWBA results obtained for different incident energies, namely E_a equal to 50 eV, 200 eV, 300 eV, and 2 keV, respectively. Acceptable agreements are found between the theoretical results and the experimental data taken from Bolorizadeh and Rudd [11] (solid circles).

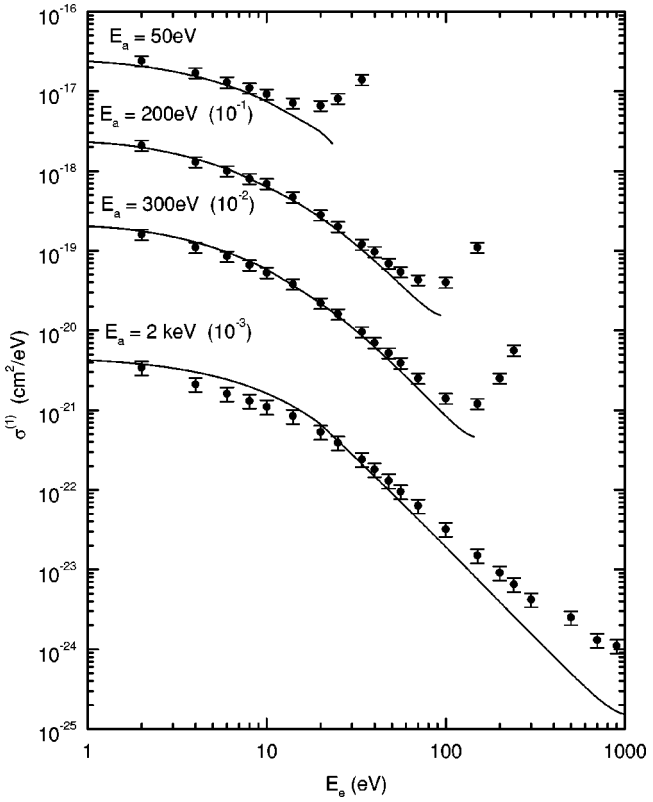

FIG. 5. SDCS's of the water-molecule ionization calculated in the DWBA framework (solid line) compared to experimental data taken from Bolorizadeh and Rudd (solid circles) in different incident energy conditions: $E_a = 50$ eV, 200 eV, 300 eV, and $E_a = 2$ keV, respectively. Multiplicative factors reported in parentheses are used for better clarity.

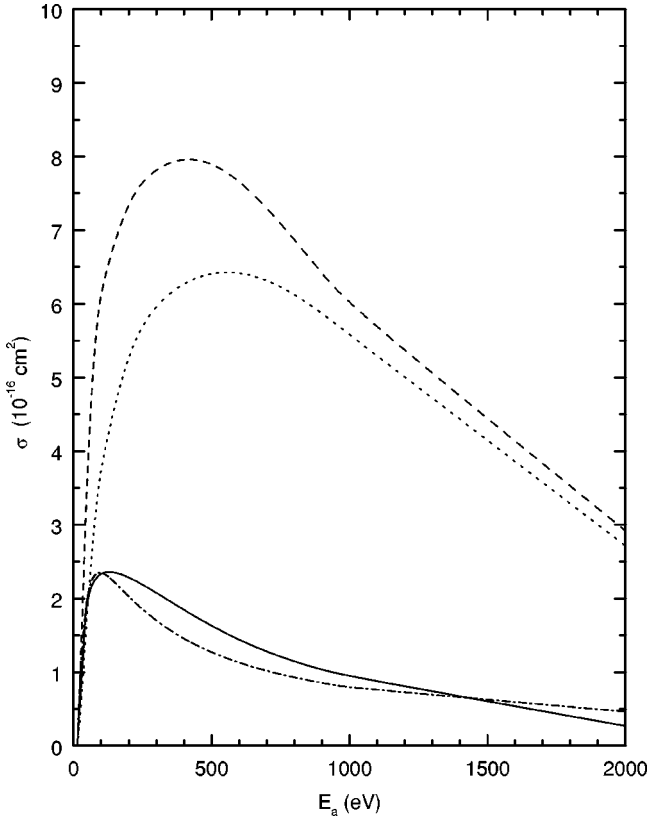

FIG. 6. Total ionization cross section σ of the vapor water molecule calculated in the DWBA framework (solid line) compared to FBA and PWBA results (dashed line and dotted line, respectively). We have reported Kim and Rudd's results (dash-dotted line).

C. Total cross sections

Total ionization cross sections σ_i are calculated for each MO labeled i by numerical integration of the SDCS's [Eq. (22)] over the energy transfers E_e from 0 to $(E_a - V_i)/2$. Then, the ''global'' TCS is obtained by summing up all the N_{orb} individual cross sections σ_i. Figure 6 displays the theoretical results obtained in the DWBA, FBA, and PWBA frameworks (solid, dotted, and dashed line, respectively) in the range 10 eV–2 keV primary electron energy, including the results of Kim and Rudd [25] (dash-dotted line). We observe that the FBA and the PWBA results overestimate the total cross sections by a factor that can reach a value of about 7 in the region $E_a < 2$ keV. The overall behavior of the curves obtained in these two frameworks is similar and the TCS values in the high-energy region tend to be identical, in the order of about $2.91 \times 10^{-16}\,\mathrm{cm}^2$ and $2.71 \times 10^{-16}\,\mathrm{cm}^2$ for $E_a = 2$ keV, respectively, i.e., six times greater than the experimental ones, which is in the order of $(0.37 \pm 0.09) \times 10^{-16}\,\mathrm{cm}^2$. Moreover, the maximal TCS value corresponds to an incident energy $E_a = 400$ and 500 eV in the FBA and PWBA frameworks, respectively, which is in large disagreement with the experiment data that display a peak centered at about $E_a = 120$ eV, which is what is in acceptable agreement with our DWBA calculations. Concerning Kim and Rudd's results [25] (dash-dotted line), they are in moderate agreement with our results, essentially in low incident energy ($E_a < 100$ eV), but display sensitive differences for greater incident energies. The discrepancies are lower than 15% in the high-incident energy range and fall off to 6% for small incident energies.

In Fig. 7 the TCS's for vapor water-molecule ionization in the incident energy range of 10 eV to 2 keV calculated in the DWBA framework (solid line) are compared to an extensive set of experimental data. The experimental ionization cross sections reported are those of Bolorizadeh and Rudd [11], Djuric *et al.* [13], Schutten *et al.* [14], Khare and Meath [16], Straub [17], and Olivero [21]. Although there exists close agreement between some of the measurements of ionization cross sections over part of the energy spectrum, there is considerable variation in the range 50 eV–1 keV. We have excluded the sets of experimental data of Gomet [22] and Orient and Srivastava [24], which deviate greatly from the other measurements. Also, we have not included results from experiments that did not provide data on an absolute scale [23]. The dotted line represents a least-squares fit to all experimental data using a model function [43].

The DWBA results are in fair agreement with the experimental data sets reported and the overall behavior of the TCS

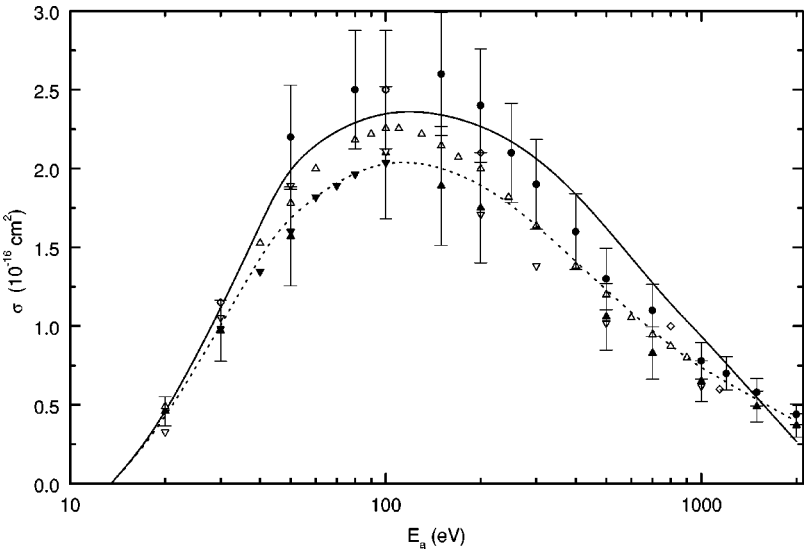

FIG. 7. Comparison between the calculated total ionization cross sections of the vapor water molecule (in the DWBA framework) and experimental data taken from various sources (Bolorizadeh and Rudd, solid circles; Djuric *et al.*, solid down triangles; Schutten *et al.*, solid up triangles; Khare and Meath, open down triangles; Straub, open up triangles; and Olivero *et al.*, open diamonds). The solid line represents the DWBA results and the dotted line a least-squares fit to all experimental data (see the text for more details).

theoretical curve is well reproduced. We observe fair agreement with the least-squares fitting curve with a maximum located at $E_a = 120$ eV.

IV. CONCLUSIONS

In the present investigation we have proposed a theoretical work dedicated to the calculation of differential and total ionization cross sections for the water-molecule target in the vapor phase. In the energy domain investigated by the present work, i.e., where the ejected energy E_e is always smaller than the scattered energy E_s, the DDCS results obtained are in fair agree-ments with the experimental data available in the literature. However, note that when E_e and E_s are comparable, the exchange will probably modify to some extent the TDCS's and the DDCS's. Concerning the SDCS results, we have obtained good agreements with the experimental set of data we have reported, which induces very good results about the total ionization cross section calculations. On the theoretical side, this work appears as an approach that permits the calculations of multiple differential cross sections of the water-molecule ionization and that can easily be introduced in numerical simulations (such as Monte Carlo simulations) of the crossing of charged particles through the biological matter, the latter being, in major part, constituted by water.

[1] F. W. Byron and C. J. Joachain, Phys. Rep. **179**, 211 (1989).
[2] I. E. Mc Carthy and E. Weigold, Rep. Prog. Phys. **54**, 789 (1991).
[3] H. Ehrhardt, K. Jung, G. Knoth, and P. Schlemmer, Z. Phys. D: At., Mol. Clusters **1**, 3 (1986).
[4] R. W. Zurales and R. R. Lucchese, Phys. Rev. A **35**, 2852 (1994).
[5] M. Cherid, A. Lahmam-Bennani, R. W. Zurales, R. R. Lucchese, A. Duguet, M. C. Dal Cappello, and C. Dal Cappello, J. Phys. B **22**, 3483 (1989).
[6] T. W. Shyn and W. Sharp, Phys. Rev. A **20**, 2332 (1979).
[7] T. W. Shyn, W. E. Sharp, and Y. K. Kim, Phys. Rev. A **24**, 79 (1981).
[8] T. W. Shyn, Phys. Rev. A **27**, 2388 (1982).
[9] M. E. Rudd, K. W. Hollman, J. K. Lewis, D. L. Johnson, R. R. Porter, and E. L. Fagerquist, Phys. Rev. A **47**, 1866 (1993).
[10] C. B. Opal, E. C. Beaty, and W. K. Peterson, At. Data **4**, 209 (1972).
[11] M. A. Bolorizadeh and M. E. Rudd, Phys. Rev. A **33**, 882 (1985).
[12] N. Oda, Radiat. Res. **64**, 80 (1975).
[13] N. Lj. Djuric, I. M. Cadez, and M. V. Kurepa, Int. J. Mass Spectrom. Ion Processes **83**, R7 (1988).
[14] J. Schutten, F. J. de Heer, H. R. Moustafa, A. J. H. Boerboom, and J. Kistenmaker, J. Chem. Phys. **44**, 3924 (1966).
[15] M. V. V. Rao, I. Iga, and S. K. Srivastava, J. Geophys. Res., [Atmos.] **100**, 26 421 (1995).
[16] S. P. Khare and W. J. Meath, J. Phys. B **20**, 2101 (1987).
[17] H. C. Straub, B. G. Lindsay, K. A. Smith, and R. F. Stebbings, J. Chem. Phys. **108**, 109 (1998).
[18] T. J. Dolan, J. Phys. D **26**, 4 (1993).
[19] K. W. Hollman, G. W. Kerby III, M. E. Rudd, J. H. Miller, and S. T. Manson, Phys. Rev. A **38**, 3299 (1988).
[20] D. A. Vroom and R. L. Palmer, J. Chem. Phys. **66**, 3720 (1977).
[21] J. J. Olivero, R. W. Stagat, and A. E. S. Green, J. Geophys. Res. **77**, 4797 (1972).
[22] J. C. Gomet, C. R. Acad. Sci., Ser. B **281**, 627 (1975).
[23] T. D. Mark and F. Egger, Int. J. Mass Spectrom. Ion Phys. **20**, 89 (1976).
[24] O. J. Orient and S. K. Srivastava, J. Phys. B **20**, 3923 (1987).
[25] Y-K. Kim and M. E. Rudd, Phys. Rev. A **50**, 3954 (1994).
[26] W. Hwang, Y-K. Kim, and M. E. Rudd, J. Chem. Phys. **104**, 2956 (1996).
[27] Y-K. Kim and M. E. Rudd, Comments At. Mol. Phys. **34**, 293 (1999).
[28] L. Vriens, in *Case Studies in Atomic Physics*, edited by E. W. McDaniel and M. R. C. McDowell (North-Holland, Amsterdam, 1969), Vol. 1, p. 335.
[29] H. Bethe, Ann. Phys. (Leipzig) **5**, 325 (1930).
[30] J. E. Turner, H. G. Paretzke, R. N. Hamm, H. A. Wright, and R. H. Ritchie, Radiat. Res. **92**, 47 (1982).
[31] D. K. Jain and S. P. Khare, J. Phys. B **9**, 1429 (1976).
[32] K. A. Long, H. G. Paretzke, F. Mller-Plathe, and G. H. F. Diercksen, J. Chem. Phys. **91**, 1569 (1989).
[33] S. P. Khare, Planet. Space Sci. **17**, 1257 (1969).
[34] S. P. Khare, J. Phys. B **3**, 971 (1970).
[35] S. P. Khare and B. D. Padalia, J. Phys. B **3**, 1073 (1970).
[36] R. Shingal, B. B. Srivastava, and S. P. Khare, J. Chem. Phys. **61**, 4656 (1974).
[37] C. Champion and A. L'Hoir (unpublished).
[38] C. Champion, J. Hanssen, and P. A. Hervieux, Phys. Rev. A **63**, 052720 (2001).
[39] R. Moccia, J. Chem. Phys. **40**, 2186 (1964).
[40] S. Uehara, H. Nikjoo, and D. T. Goodhead, Phys. Med. Biol. **37**, 1841 (1992).
[41] M. A. Coplan, J. H. Moore, and J. P. Doering, Rev. Mod. Phys. **66**, 985 (1994).
[42] N. F. Mott and H. S. W. Massey, in *The Theory of Atomic Collisions*, 3rd ed., edited by W. Marshall and D. H. Wilkinson (Oxford, Clarendon Press, 1971), p. 858.
[43] S. Uehara, H. Nikjoo, and D. T. Goodhead, Radiat. Res. **152**, 202 (1999).